DTIC COPY

REPORT DOCUMENTATION PAGE

Form Approved
OMB No. 0704-01-0188

PLEASE DO NOT RETURN YOUR FORM TO THE ABOVE ADDRESS.

1. REPORT DATE (DD-MM-YYYY)	2. REPORT TYPE	3. DATES COVERED (From - To)
05-07-2007	REPRINT	

4. TITLE AND SUBTITLE

Refractive index and wavenumber properties for cyclotron resonant quasilinear diffusion by cold plasma waves

5a. CONTRACT NUMBER

5b. GRANT NUMBER

5c. PROGRAM ELEMENT NUMBER
62601F

6. AUTHORS
J.M. Albert

5d. PROJECT NUMBER
1010

5e. TASK NUMBER
RR

5f. WORK UNIT NUMBER
A1

7. PERFORMING ORGANIZATION NAME(S) AND ADDRESS(ES)

Air Force Research Laboratory /RVBXR
29 Randolph Road
Hanscom AFB, MA 01731-3010

8. PERFORMING ORGANIZATION REPORT NUMBER
AFRL-RV-HA-TR-2008-1011

9. SPONSORING/MONITORING AGENCY NAME(S) AND ADDRESS(ES)

10. SPONSOR/MONITOR'S ACRONYM(S)
AFRL/RVBXR

11. SPONSOR/MONITOR'S REPORT NUMBER(S)

12. DISTRIBUTION/AVAILABILITY STATEMENT
Approved for Public Release; distribution unlimited.

13. SUPPLEMENTARY NOTES
Reprinted from *Physics of Plasmas,* Vol. 14, 072901 (2007) doi:10.1063/1.2744363

14. ABSTRACT

Wave-particle interactions have a large effect on magnetospheric particles, in the radiation belts and elsewhere. Bounce-averaged quasilinear diffusion coefficients have been calculated for whistler hiss and chorus and electromagnetic ion cyclotron waves (EMIC), which are all believed to play major roles. To perform these calculations efficiently, techniques have been developed that use properties of the refractive index of these modes to identify ranges of wave-normal angle that are compatible with cyclotron resonance in a given frequency band. Other cold plasma waves, in the L-X, L-O, R-X, and Z modes, can also resonate with energetic electrons, and some preliminary calculations of their diffusion coefficients have been reported. Here, it is shown that the refractive index of these modes allows the techniques developed for whistler and EMIC waves to applied to them as well. Sample calculations are presented for Z mode waves, with $\omega_{pe}>\Omega_e$ and $\omega_{pe}<\Omega_e$. It is also observed that for any cold plasma mode, the wavenumber is an increasing function of frequency for a fixed value of wave-normal angle; this is proved algebraically with mild approximations and verified numerically for a very wide range of parameters. This allows a variant of the technique for efficiently calculating diffusion coefficients.

15. SUBJECT TERMS
Pitch angle diffusion Radiation belts

16. SECURITY CLASSIFICATION OF:			17. LIMITATION OF ABSTRACT	18. NUMBER OF PAGES	19a. NAME OF RESPONSIBLE PERSON
a. REPORT	b. ABSTRACT	c. THIS PAGE			J. M. Albert
UNCL	UNCL	UNCL			19B. TELEPHONE NUMBER (Include area code)

PHYSICS OF PLASMAS 14, 072901 (2007)

Refractive index and wavenumber properties for cyclotron resonant quasilinear diffusion by cold plasma waves

J. M. Albert
Air Force Research Laboratory/VSBX, Hanscom AFB, Massachusetts 01731, USA

(Received 20 December 2006; accepted 8 May 2007; published online 5 July 2007)

Wave-particle interactions have a large effect on magetospheric particles, in the radiation belts and elsewhere. Bounce-averaged quasilinear diffusion coefficients have been calculated for whistler hiss and chorus and electromagnetic ion cyclotron waves (EMIC), which are all believed to play major roles. To perform these calculations efficiently, techniques have been developed that use properties of the refractive index of these modes to identify ranges of wave-normal angle that are compatible with cyclotron resonance in a given frequency band. Other cold plasma waves, in the L-X, L-O, R-X, and Z modes, can also resonate with energetic electrons, and some preliminary calculations of their diffusion coefficients have been reported. Here, it is shown that the refractive index of these modes allows the techniques developed for whistler and EMIC waves to be applied to them as well. Sample calculations are presented for Z mode waves, with $\omega_{pe} > \Omega_e$ and $\omega_{pe} < \Omega_e$. It is also observed that for any cold plasma mode, the wavenumber is an increasing function of frequency for a fixed value of wave-normal angle; this is proved algebraically with mild approximations and verified numerically for a very wide range of parameters. This allows a variant of the technique for efficiently calculating diffusion coefficients. [DOI: 10.1063/1.2744363]

I. INTRODUCTION

Cyclotron-resonant wave-particle interactions are crucial to the dynamics of magnetospheric particles, particularly radiation belt electrons. Whistler mode hiss within the plasmasphere, whistler mode chorus outside the plasmasphere, and electromagnetic ion cyclotron (EMIC) waves at the plasmapause or within density plumes are all believed to play major roles. Their quantitative effects have recently been calculated in detail,[1–6] using bounce-averaged local quasilinear theory.[7,8] In the low-density region outside the plasmasphere, electrons are also capable of resonant interactions with the cold plasma L-X, L-O, R-X, and Z modes.[9,10] Preliminary calculations of diffusion coefficients for these modes have also recently been presented.[5,11]

The full bounce-averaged quasilinear calculations are fairly demanding, since even local diffusion coefficients involve integration over a continuum of waves, requiring the resonant frequency for each wave-normal angle or vice versa, compounded by the sum over resonant harmonic number n (in principle, from $-\infty$ to ∞). When bounce averaging is performed, it becomes impractical to repeat the calculations for many different values of particle energy and equatorial pitch angle, background density, and wave parameters. To circumvent this, simplified forms of the local diffusion coefficients have been derived assuming parallel propagating waves,[12] and bounce averaged and found to give good estimates of the exact results for chorus waves in several test cases.[13] A different approach is to identify in advance, and eliminate, integration ranges that are incompatible with cyclotron resonance for the given wave population. This greatly reduces the amount of computation required without changing the result, provides a rational criterion for limiting the range of n, and provides insight into which waves contribute to the diffusion (which suggests an approach for parameter sensitivity studies). Such techniques have previously been developed for whistler mode hiss,[1] EMIC,[2] and chorus,[3] based on detailed analysis of the refractive index of these wave modes. Here, it is shown how they may be easily applied to L-X, L-O, R-X, and Z mode electromagnetic waves as well.

Also discussed is a closely related approach based on the behavior of the wavenumber, k, rather than refractive index, kc/ω, for cold plasma waves. It is shown in general that k is an increasing function of frequency ω, at a fixed wave-normal angle θ. This basic observation about $k(\omega)$ does not seem to have received as much attention as $k(\theta)$ has. Here this property is established theoretically as far as possible, and numerically in general, to justify its use in calculating diffusion coefficients.

II. WAVE MODES

All of the cold plasma wave modes are given by the standard expression for the refractive index,[14]

$$\Psi_\pm = \frac{\omega^2}{k_\pm^2 c^2} = \{(RL - PS)\sin^2\theta + 2PS \pm \sigma\sqrt{(RL - PS)^2 \sin^4\theta + 4P^2D^2\cos^2\theta}\}/2PRL, \tag{1}$$

where the quantities (R, L, P, S, D) depend on the wave, cyclotron, and plasma frequencies (ω, Ω, and ω_p, respectively), and σ is defined to be $+1$ for $PD > 0$ and -1 for $PD < 0$. The ω dependence for a pure hydrogen plasma is shown in Fig. 1 for $\omega_{pe}^2/\Omega_e^2 = 0.3$ and $\omega_{pe}^2/\Omega_e^2 = 2.2$ (representative of background plasma with mildly low and mildly high density, respectively), for several values of θ. Also shown are the limiting cases $\Psi_-(\theta = 0) = 1/R$, $\Psi_+(\theta = 0) = 1/L$, and $\Psi_+(\theta$

1070-664X/2007/14(7)/072901/8/$23.00

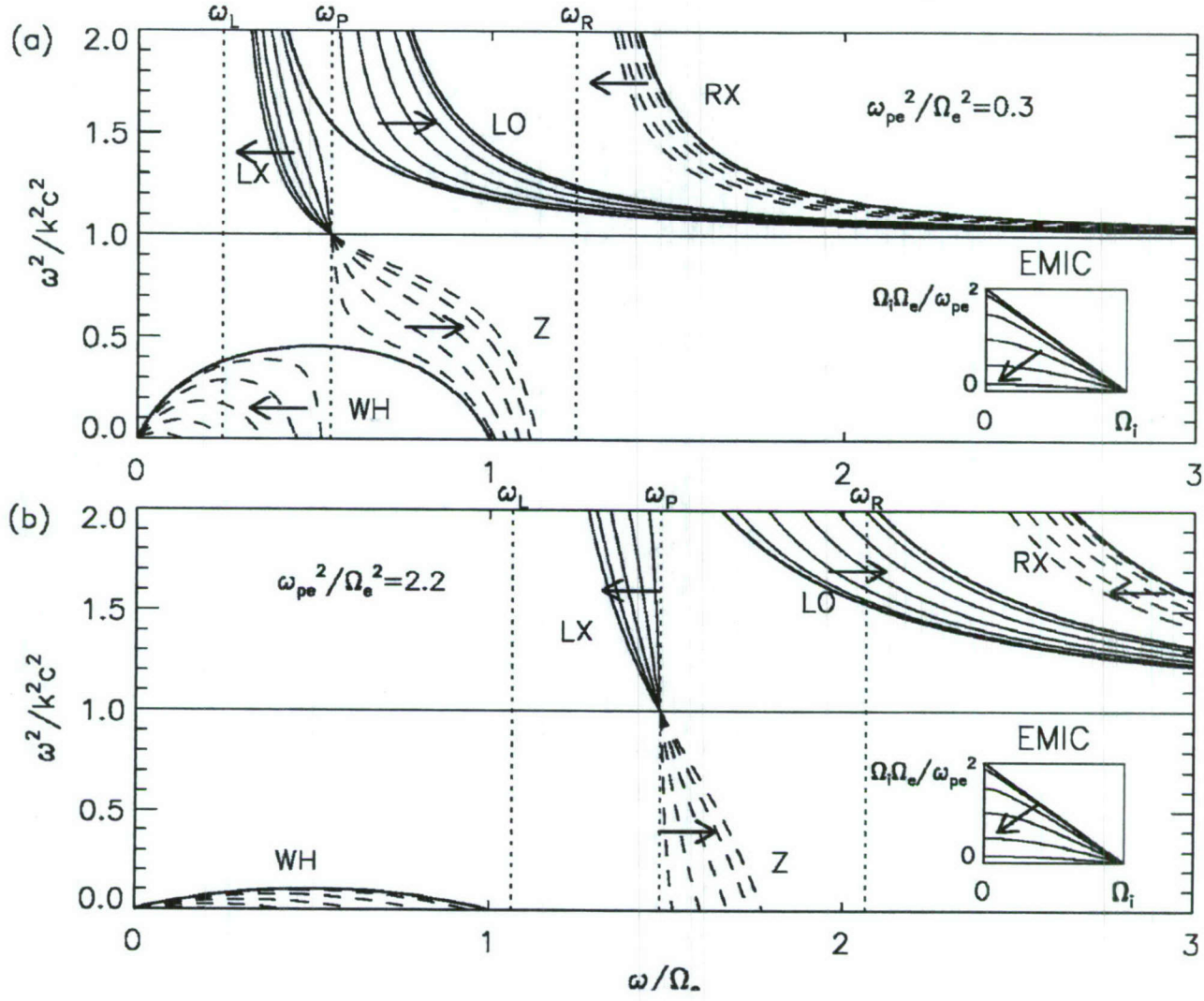

FIG. 1. The functions $\Psi_\pm=\omega^2/k_\pm^2c^2$ vs ω/Ω_e for a pure hydrogen plasma, with $\theta=15°, 30°, 45°, 60°, 75°$. The superluminous L-X, L-O, and R-X modes, and the whistler and Z modes are shown with solid curves for the Ψ_+ branches and dashed curves for Ψ_-. The thick curves with $\Psi>1$ are $1/L$, $1/P$, and $1/R$ (left to right, respectively); the thick curve with $\Psi<1$ is also $1/R$. The insets show Ψ_+ vs ω/Ω_i for the same parameters; the thick curve is $1/L$, with maximum value $\approx\Omega_i\Omega_e/\omega_{pe}^2$ at $\omega=0$. For each wave mode in the top panel, the arrows show the direction of increasing θ.

$=90°)=1/P$, as well as the frequencies ω_L, $\omega_P=\omega_{pe}$, and ω_R at which L, P, and R are zero, respectively. The branches above the line $\omega^2/k^2c^2=1$ are superluminous, with phase velocity $\omega/k>c$. Finally, the insets show Ψ_+ for $0<\omega<\Omega_i$, which are EMIC waves.

With the heavy-ion or magneto-ionic approximation $m_e/m_i=0$ in the definitions of R, L, and P, Eq. (1) can be written in the form

$$\Psi_\pm=[1-1/(A\hat{\omega}^2\Delta_\pm)]^{-1},$$
$$\Delta_\pm=1-\frac{A\sin^2\theta}{2(A\hat{\omega}^2-1)}\pm\sqrt{\frac{A^2\sin^4\theta}{4(A\hat{\omega}^2-1)^2}+\frac{\cos^2\theta}{\hat{\omega}^2}}, \quad (2)$$

where $\hat{\omega}=\omega/\Omega_e$ and $A=\Omega_e^2/\omega_{pe}^2$. Also, $\omega_{R,L}=\Omega_e[(1+4/A)^{1/2}\pm1]/2$ and $\omega_P=\Omega_e/A^{1/2}$. Note that $\omega_L<\omega_P<\omega_R$, and that $\omega_L\gg\Omega_i$ as long as $\omega_{pe}^2/\Omega_e^2\gg m_e/m_i$. Positive Ψ requires either $A\omega^2\Delta>1$ (superluminous modes) or $\Delta<0$ (subluminous modes).

The three superluminous modes are identified[10] as the L-X, with $\omega_L<\omega<\omega_P$ and described by Ψ_+; the L-O, with $\omega>\omega_P$ and described by Ψ_+; and the R-X, with $\omega>\omega_R$ and described by Ψ_-. Also shown are the subluminous whistler and Z modes, given by Ψ_-. The whistler mode has $\omega<\min[\Omega_e,\omega_P]$, while the Z mode propagates for ω between ω_P and the upper hybrid frequency ω_{UH}, defined by $S=0$. This lies below ω_R since, in the magneto-ionic approximation, $\omega_{UH}=\Omega_e(1+1/A)^{1/2}$ so that $\omega_R^2-\omega_{UH}^2=\omega_L\Omega_e>0$.

Both whistler and Z-mode propagation can be subject to a resonance cone, given by $\tan^2\theta_{RC}=-P/S\approx(\omega_{pe}^2-\omega^2)(\Omega_e^2-\omega^2)/(\omega_{UH}^2-\omega^2)\omega^2$, assuming $\omega>\omega_{LH}\approx(\Omega_i\Omega_e)^{1/2}$. Propagation then requires $\theta<\theta_{RC}$. Z-mode waves will have a resonance cone when $\omega>\Omega_e$, requiring $\theta>\theta_{RC}$ for propagation; this is necessarily the case when $\omega_{pe}/\Omega_e>1$.

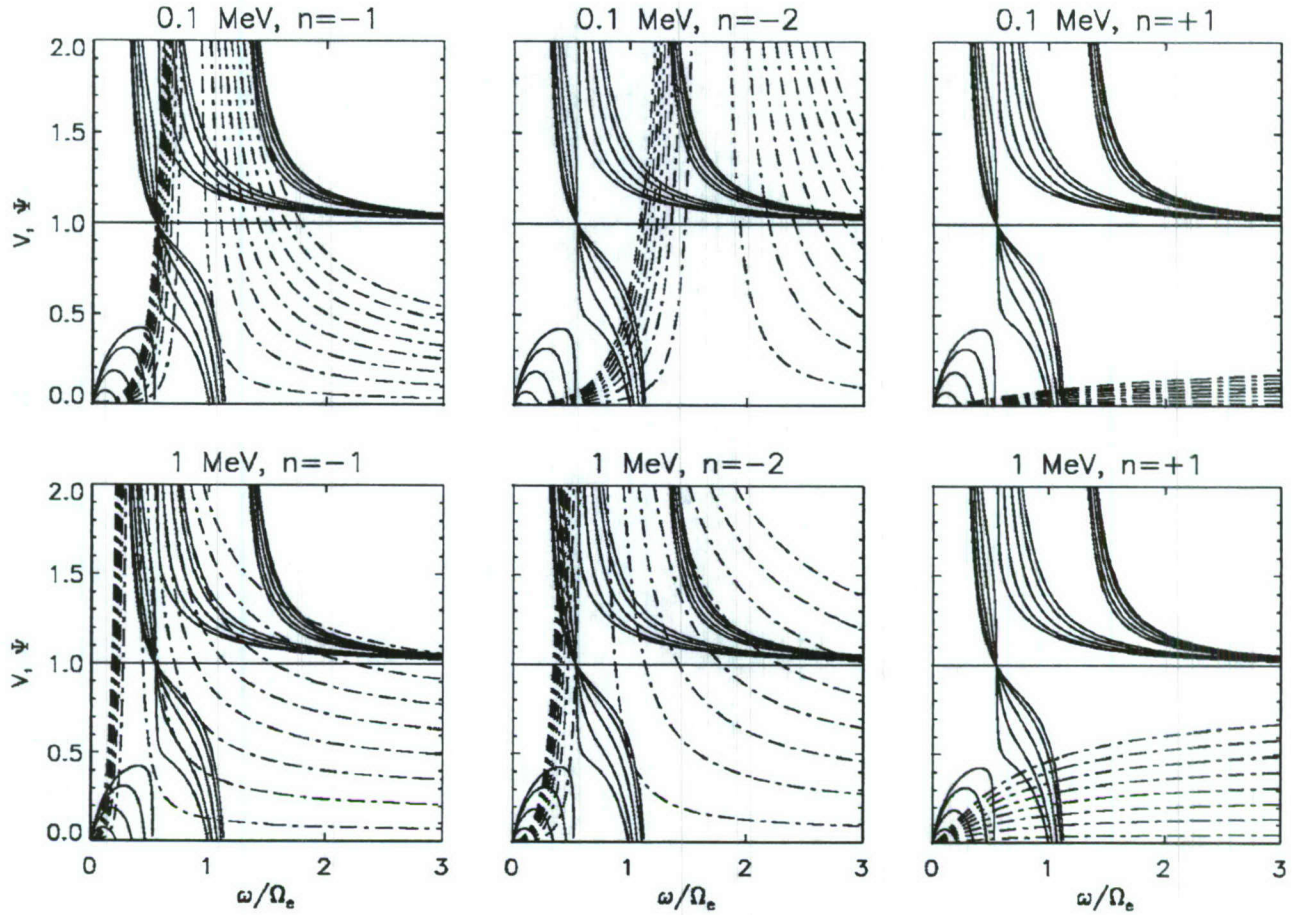

FIG. 2. The functions Ψ (solid curves) and V (dashed curves) with $\omega_{pe}^2/\Omega_e^2=0.3$, wave-normal angle θ from 0 to 90°, and pitch angle α from 0 to 90°, for $n=-1$, -2, and $+1$. Cyclotron resonance occurs where $V=\Psi$.

III. DIFFUSION COEFFICIENTS AND RESONANCES

To implement the quasilinear formulation, the wave population is usually modeled by the product of Gaussian distributions of frequency and wave-normal angle (θ or $x=\tan\theta$), with sharp cutoffs for each.[7,8] The local diffusion coefficients (for pitch angle, momentum, and cross diffusion) have the form of sums of integrals over θ from a minimum to a maximum value,

$$D=\sum_{n=-\infty}^{\infty}\int_{\theta_{\min}}^{\theta_{\max}}\mathcal{D}_n(\theta,\omega)d\theta. \tag{3}$$

Here ω is the resonant frequency corresponding to n and θ, given by

$$\omega-k_\parallel v_\parallel=\omega_n,\quad \omega_n\equiv sn\Omega_c/\gamma, \tag{4}$$

where Ω_c is the nonrelativistic, unsigned cyclotron frequency of the diffusing test particle and $s=q/|q|$. $\mathcal{D}_n$ is taken to be zero unless ω lies between lower and upper cutoffs ω_{LC} to ω_{UC}. Within the cutoffs, the distributions may be parametrized by peak and half-width values,[7] e.g., $(\theta_m,\theta_w;\omega_m,\delta\omega)$. The permissible frequency range depends on the wave mode being studied, but the range actually used constitutes an empirical model of the waves and may be much narrower. (Since the local diffusion coefficients involve ranges of ω but keep Ω_e and ω_{pe} fixed, it may be useful to redraw[15] the CMA diagram delineating the various wave modes, with axes ω_{pe}^2/Ω_e^2 and ω/Ω_e rather than the conventional quantities ω_{pe}^2/ω^2 and Ω_e/ω).

The cyclotron resonance condition can be written as

$$\Psi\equiv\frac{\omega^2}{k^2c^2}=\frac{\omega^2}{(\omega-\omega_n)^2}\frac{v^2}{c^2}\cos^2\alpha\cos^2\theta\equiv V. \tag{5}$$

This includes resonances with both signs of $k_\parallel v_\parallel$, which is justified if the upgoing and downgoing wave populations are assumed equal, or if both halves of the particle's bounce motion are considered.

Figure 2 shows $V(\omega)$ and $\Psi(\omega)$ for $\omega_{pe}^2/\Omega_e^2=0.3$, for a wide range of θ and α. The Ψ curves are the same in each panel [and the same as in Fig. 1(a)], while V, which decreases as θ increases, is shown for different values of energy and n. Generally speaking, with $n=-1$ resonances are readily found for the L-X and L-O modes (as well as the whistler and Z modes) but are marginal for the R-X mode, in agreement with Ref. 10. However, with $n=-2$, resonances are also plentiful for the R-X mode over a broad range of parameters, as are resonances with $n>0$ for the whistler and Z modes.

To recap the calculation method of Refs. 1–3, the idea is

to identify the ranges of θ within $\theta_{\min}$ to $\theta_{\max}$ for which ω lies outside ω_{LC} to ω_{UC}, and exclude them before performing the integrations. To this end, each side of Eq. (5) is considered geometrically as a function of ω at fixed θ. The minimum and maximum values of $V(\omega)$ over ω_{LC} to ω_{UC} are readily determined. For example, with $\omega_n<0$, $V(\omega)$ is monotonically increasing so $V_{\min}=V(\omega_{LC})$ and $V_{\max}=V(\omega_{UC})$. If the minimum and maximum values of Ψ can be characterized as well, then θ ranges are disqualified according to the simple criteria

$$V_{\min} > \Psi_{\max} \text{ or } V_{\max} < \Psi_{\min}. \tag{6}$$

These conditions are easily interpreted graphically by drawing a rectangle defined by ($\omega_{LC} \leqslant \omega \leqslant \omega_{UC}$, $\Psi_{\min} \leqslant \Psi \leqslant \Psi_{\max}$). The $V(\omega)$ and $\Psi(\omega)$ curves can only intersect for θ such that V passes through this rectangle; other ranges of θ need not be considered. An extreme instance of this is that superluminous modes have $\Psi_{\min}>1$ while $V_{\max}<1$ for $\omega_n \leqslant 0$, so there are no superluminous resonances with $\omega_n \leqslant 0$ (i.e., with $n \geqslant 0$ for electrons). Algebraically, conditions (6) are easily solved quadratic inequalities[1,2] for $\sin^2\theta$. Excluding the corresponding θ ranges greatly reduces the amount of work required to evaluate the diffusion coefficients, particularly since for $|n|$ sufficiently large, no θ values remain at all.

The success of the method depends on being able to find (or bound) the minimum and maximum values of $\Psi(\omega)$ for fixed θ. This is especially simple if $\Psi(\omega)$ behaves monotonically, as Fig. 1 suggests often occurs. As noted above, this has already been studied in detail for chorus mode and EMIC waves. In the following subsections, the behavior of $\Psi(\omega)$ is investigated for the superluminous and Z modes.

A. Superluminous modes

From Eq. (2), the sign of the slope $\Psi' = \partial\Psi/\partial\omega$ for the superluminous modes is given by

$$\Psi'_{\pm} \sim -(\omega^2\Delta'_{\pm} + 2\omega\Delta_{\pm}). \tag{7}$$

Then it is straightforward to show that $\Psi'_{+}<0$, so that $\Psi'<0$ for both the L-X and L-O modes. For the R-X mode, it can be shown that $\Delta'_{-}>0$ for $\omega>\omega_R$ (or even for the less demanding condition $\omega>\omega_P$). It is also easily checked that $\Delta_{-}>0$ at ω_R, and therefore at $\omega>\omega_R$, so that $\Psi'<0$ holds for the R-X mode as well. Thus conditions (6) may be exploited for superluminous waves just as it was for EMIC waves.[2]

B. Z mode

Figure 3 shows Ψ for the whistler and Z modes with $\omega_{pe}^2/\Omega_e^2=0.1$ and $\theta=1°,2°,3°$. It is evident that the Z mode does not strictly obey $\Psi'(\omega)>0$ for $\omega<\Omega_e/2$, where $1/R(\omega)$ is increasing, if θ is small enough that $\Psi \approx 1/R$. Such Z mode waves require $\omega_{pe}<\omega<\Omega_e/2$, or $\omega_{pe}/\Omega_e<0.5$. It is conjectured that this behavior is controlled by the sign of Ψ'' evaluated at $\Omega_e/2$, just as Ψ'' evaluated at $\omega=0$ was seen[3] to control the behavior of the whistler mode for very small ω and large θ. (Perhaps fortuitously, the numerical example of Ref. 5 takes $\omega_{pe}/\Omega_e=0.5$ and $\omega_{LC}/\Omega_e=0.55$).

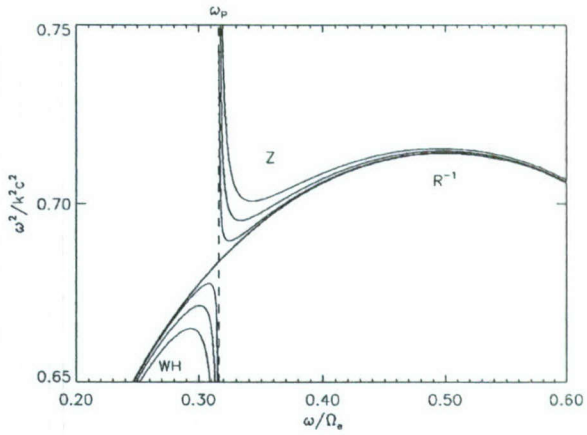

FIG. 3. The function $\Psi_{-}=\omega^2/k_{-}^2c^2$ vs ω/Ω_e for the whistler and Z modes, with $\Omega_e^2/\omega_{pe}^2=0.1$ and $\theta=1°,2°,3°$. Also shown is the value for $\theta=0$, namely $1/R$.

1. Estimates of $\Psi_{\max}$ and $\Psi_{\min}$

To characterize the behavior of $\Psi(\omega)$ in the problematic cases, we turn to a factorization found for the whistler mode, $\Psi=\Psi_1\Psi_2$, where

$$\Psi_1 = \frac{D}{R}\frac{\omega}{\Omega_e},$$
$$\Psi_2 = \frac{\Omega_e}{\omega L}\left\{\frac{(RL-PS)\sin^2\theta + 2PS}{2PD} - \sqrt{\frac{(RL-PS)^2\sin^4\theta}{4P^2D^2} + \cos^2\theta}\right\}. \tag{8}$$

For $\omega^2>\Omega_e\Omega_i$, Ψ_1 is an increasing function of ω while Ψ_2 is a decreasing function of ω; a proof was outlined in Ref. 16. (Walker,[17] in a related context, refers to "the horrendous algebra involved.") A careful review of that proof shows that it holds for the Z mode as well. Thus the bounds

$$\Psi_1(\omega_{LC})\Psi_2(\omega_{UC}) < \Psi(\omega) < \Psi_1(\omega_{UC})\Psi_2(\omega_{LC}) \tag{9}$$

may be exploited for Z mode waves just as it recently was for whistler waves.[3] Actually, if $\omega_{LC}<\Omega_e/2<\omega_{UC}$, treating the two subintervals separately gives the tighter bounds

$$\min[\Psi_1(\omega_{LC})\Psi_2(\Omega_e/2), \Psi(\omega_{UC})] < \Psi(\omega) < \max[\Psi_1(\omega_{UC})\Psi_2(\Omega_e/2), \Psi(\Omega_e/2)]. \tag{10}$$

Thus one may safely skip θ ranges for which both $V_{\min}>\Psi_1(\omega_{UC})\Psi_2(\omega_{LC})$ and $V_{\min}>\Psi(\Omega_e/2)$ hold, as well as θ ranges which satisfy both $V_{\max}<\Psi_1(\omega_{LC})\Psi_2(\omega_{UC})$ and $V_{\max}<\Psi(\omega_{UC})$.

Yet another estimate of $\Psi_{\min}$ and $\Psi_{\max}$ for the Z mode comes from the observation that $\Psi(\omega)$ increases with increasing θ. To prove this, one can show in the magneto-ionic approximation that $\Psi_1>0$ for $\omega<\omega_R$ and that $\partial\Psi_2/\partial\theta$ has the same sign as L does, namely positive for the Z mode. Thus Ψ is bounded by $\min[\Psi(\omega,\theta_{\min})]$ and $\max[\Psi(\omega,\theta_{\max})]$, which may be found numerically and exploited in Eq. (6).

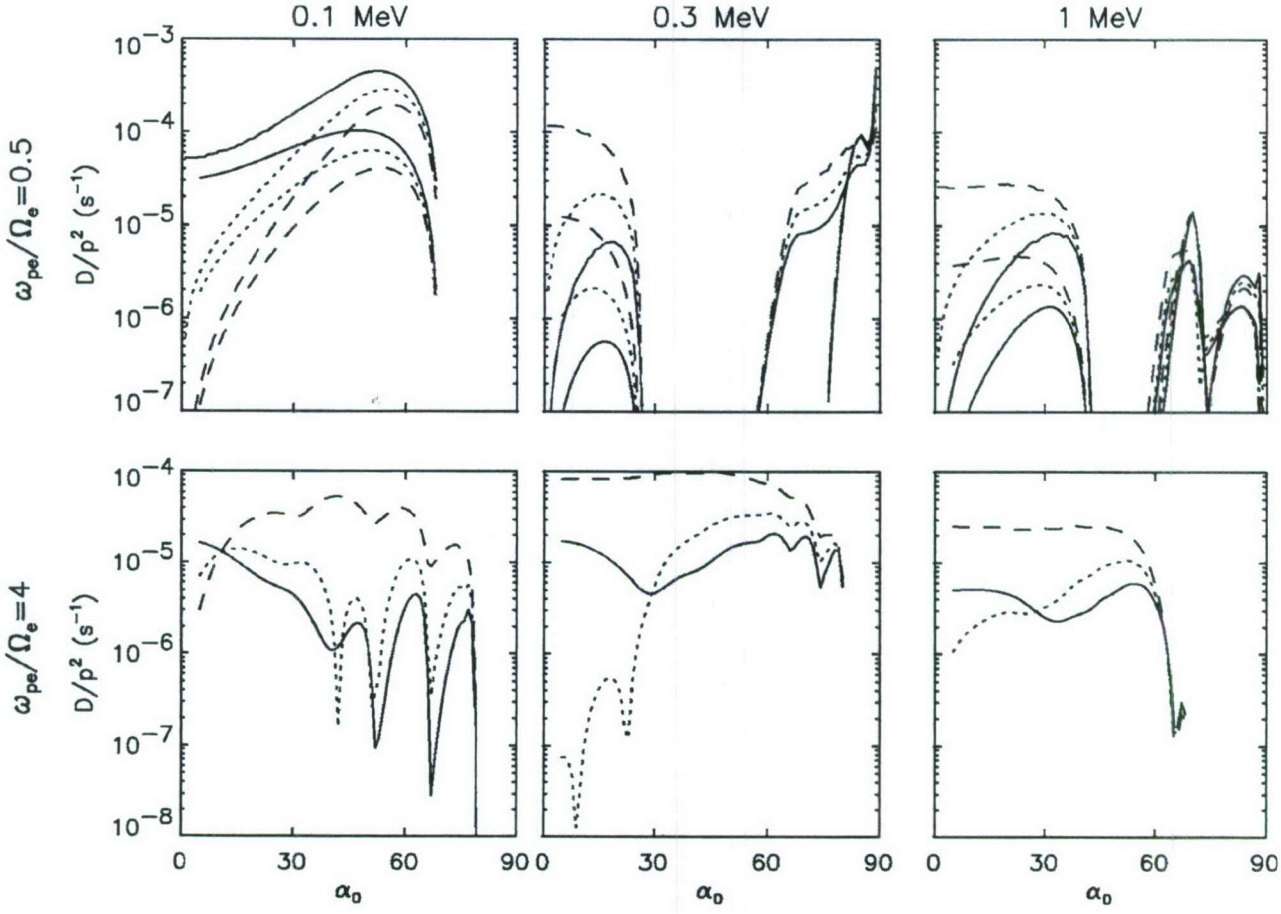

FIG. 4. Diffusion coefficients for 10 pT Z-mode waves within 10° of the equator. The top row shows equatorial and bounce-averaged pitch angle (solid curves), momentum (dashed), and cross (dotted) diffusion coefficients for $\omega_{pe}/\Omega_e=0.5$ at the equator. The local values generally lie above the corresponding bounce-averaged quantities. The bottom row shows bounce-averaged diffusion coefficients for $\omega_{pe}/\Omega_e=4$ at the equator.

2. Numerical results

Figure 4 shows diffusion coefficients for electrons interacting with Z-mode waves at $L=4.5$. The same wave model parameters are used as for the local equatorial calculations of Ref. 5, namely $\omega_{pe}/\Omega_e=0.5$, with frequency parameters $(\omega_m, \delta\omega, \omega_{LC}, \omega_{UC})=(0.60, 0.05, 0.55, 0.65)\Omega_e$ and wave-normal angle parameters $(\theta_m, \theta_w, \theta_{min}, \theta_{max})=(0, 30°, 0, 45°)$, as well as wave amplitude 10 pT. The top row of Fig. 4 shows both local equatorial and bounce-averaged diffusion coefficients; the latter took Z-mode waves to be present only for latitude within 10° of the equator (with constant ω_{pe} and dipolar variation of Ω_e). The local values replicate the values of Ref. 5 (when appropriately scaled to 100 pT), while the bounce-averaged results are significantly smaller. For 0.1 MeV, $D_{\alpha_0\alpha_0}$ is less than D_{pp} but for higher energy the reverse is generally true. Also, the waves seem ineffective for intermediate pitch angles,[5] with implications for the resulting particle distribution. However, such conclusions depend on the parameter choices, as shown in the bottom row of Fig. 4. Here $\omega_{pe}/\Omega_e=4$, with $(\omega_m, \delta\omega, \omega_{UC}, \omega_{UC})=(4.02, 1.0, 4.01, 4.025)\Omega_e$ and $(\theta_m, \theta_w, \theta_{min}, \theta_{max})=(50°, 50°, 30°, 80°)$. The frequency cutoffs span about 140 Hz, centered near 38 kHz. For larger ω_{pe}/Ω_e, the restrictions on frequency and wave-normal angle start to become prohibitive. Nevertheless, the diffusion coefficients shown are substantial over a large range of pitch angle, and the momentum rates can be larger than the pitch angle rates, a feature expected at low pitch angle for waves with $\omega > \Omega_e$.[8] For the amplitude assumed, the rates are comparable to values computed for other waves,[19] though localization of the waves in longitude has not been accounted for. Apparently Z-mode waves, if present under favorable conditions, are capable of resonating effectively with radiation belt electrons.

IV. VARIANT OF THE METHOD BASED ON WAVENUMBER

The resonance condition may also be written as

$$kc = |\omega - \omega_n|(c/v)\sec\alpha \sec\theta \equiv \Omega_e W, \tag{11}$$

again keeping both signs of $k_\parallel v_\parallel$. (At a fixed location, Ω_e is constant and just serves to normalize W.) Figure 5, analogous to Fig. 1, suggests that k, or $k^2c^2=\omega^2/\Psi$, is an increasing function of ω at fixed θ for all of the cold plasma wave modes. This is supported below. [This monotonic behavior was shown in a similar, comprehensive set of plots by Walker[18] (Figs. 3-18 to 3-20) but not remarked upon, although "contemplation" of these and related figures was rec-

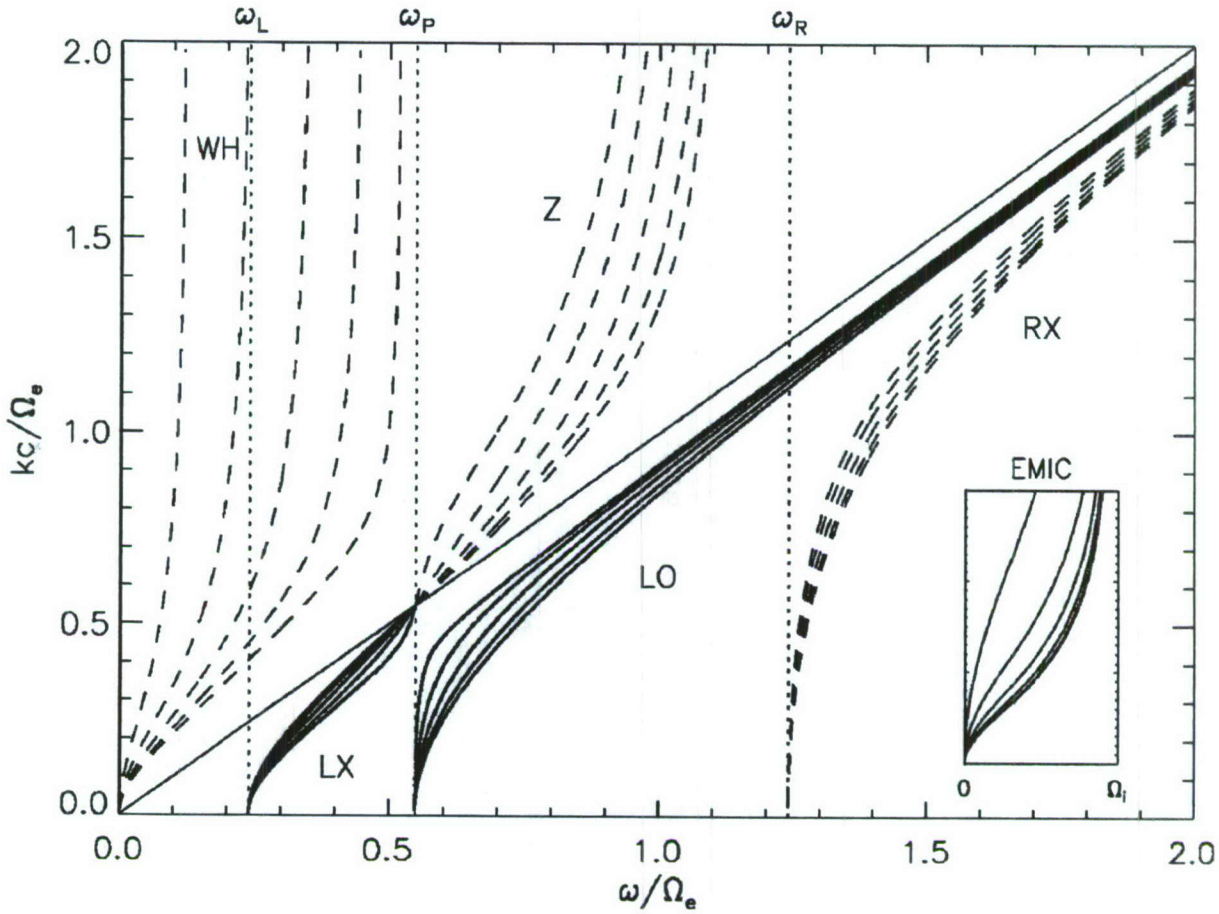

FIG. 5. The functions $k_{\pm}^2c^2/\Omega_e^2$ vs ω/Ω_e as in Fig. 1(a). The diagonal line separates the superluminous from the subluminous modes.

ommended.] This behavior immediately suggests conditions analogous to those in Eq. (6) to rule out resonances in a given frequency range,

$$W_{\min} > (kc)_{\max}/\Omega_e \text{ or } W_{\max} < (kc)_{\min}/\Omega_e, \tag{12}$$

where $(kc)_{\min}$ is evaluated at ω_{LC} and $(kc)_{\max}$ is evaluated at ω_{UC}. As before, this leads to simple quadratic equations for $\sin^2\theta$. The following subsections verify the property $(k^2)' > 0$ for the various wave modes.

A. Superluminous and EMIC waves

For the superluminous modes in the magneto-ionic approximation, ω^2/k^2c^2 has been shown to be a decreasing function of ω so obviously $1/k^2c^2$ is a decreasing function of ω and k^2c^2 is increasing. The same holds for EMIC waves, even in multispecies plasmas, in the high-density approximation.[2]

B. Z mode

For the Z mode, the sign of the slope of k^2 is given by

$$(k_-^2)' \sim 2A\omega^2\Delta_-^2 + \Delta_-' \tag{13}$$

and, as noted for the R-X mode in Sec. III A, $\Delta_-' > 0$ when $A\omega^2 - 1 > 0$ (which is guaranteed by $\omega > \omega_P$). Thus $(k^2)' > 0$ for the Z mode.

C. Whistler mode

To analyze $(k^2)'$ for the whistler mode, we resort to the factorization discussed in Sec. III B, $\Psi = \Psi_1\Psi_2$ or $k^2c^2 = (\omega^2/\Psi_1)/\Psi_2$. Since Ψ_2 is a decreasing function of ω for $\omega^2 > \Omega_i/\Omega_e$, to show that k^2 is increasing it is sufficient to show that ω^2/Ψ_1 is increasing. This expression is just $\omega R/D$, which is indeed found to have positive slope given the whistler mode properties $\omega < \Omega_e$ and $\omega < \omega_P$.

D. Numerical tests

Cases not covered above include R mode (whistler) waves with $\omega^2 < \Omega_e\Omega_i$ and EMIC waves without the high-density approximation. It is worth recalling the remarks of Stix[14] that "it is not difficult for a problem in plasma waves to become completely unwieldy. Even the simple case of waves in a cold drift-free homogeneous plasma is on the borderline of tractability," and although "the difficult problems in plasma waves in a homogeneous medium become, for the most part, just difficult problems in algebra,... the algebra is not trivial." Even the limiting case $\theta = 0$ has pitfalls: $(k_+^2c^2)' = (\omega^2 L)'$ can in fact be negative for $\Omega_i < \omega < \omega_L$, but no such waves propagate because L itself is negative in that range.

To test the observation $(k^2)' > 0$ in full generality, extensive numerical tests were performed as follows. Both $k_{\pm}^2$ and

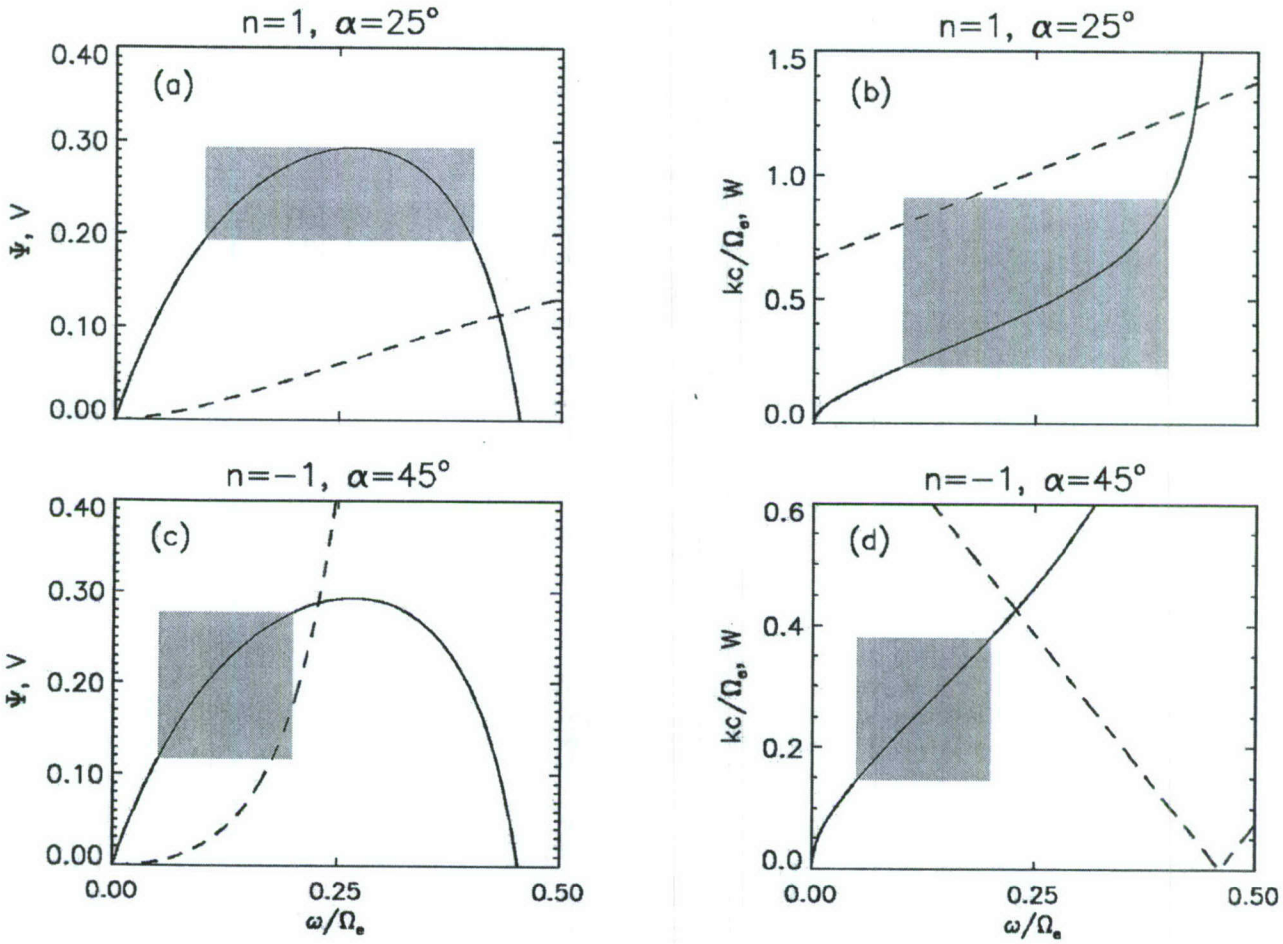

FIG. 6. Illustrations of two versions of the no-resonance criteria, for whistler waves and 600 keV electrons; other parameters are given in the text. Resonances occur where the curves intersect. (a) Because the curve of $V(\omega)$ (dashed) does not cross the rectangle determined by the minimum and maximum values of Ψ (solid curve), conditions (6) are met, indicating no resonance within the frequency cutoffs. (b) For the same parameters as (a), the curve of $W(\omega)$ (dashed) does cross the rectangle determined by the minimum and maximum values of kc/Ω_e (solid curve), so conditions (12) do not rule out resonances within the cutoffs. (c) V and $\Psi(\omega)$ for a different set of parameters. Here, since the V curve crosses the Ψ rectangle, conditions (6) do not rule out resonances within the cutoffs, though none are present. (d) For the same parameters as (c), W avoids the kc/Ω_e rectangle, so conditions (12) successfully identify the absence of resonances within the frequency cutoffs.

$(k_{\pm}^2)'$ were calculated for 1000 values of $A=\Omega_e^2/\omega_{pe}^2$ logarithmically spaced between 0.01 and 10^8, 200 uniformly spaced values $0\leq\sin^2\theta\leq 1$, and 5000 uniformly spaced frequencies $0<\omega<2\omega_R$. This wide range of A, corresponding to $10^{-4}\leq\omega_{pe}/\Omega_e\leq 10$, includes the extremely low-density range $\omega_{pe}<\Omega_i$; the frequency range $\omega<\Omega_i$ is also resolved. (Evaluating these 10^9 cases took only a few minutes on a moderately fast computer, which is one way to attack the tractability problem; algebraic manipulation software can also be useful.) A multispecies plasma (85% H^+, 5% He^+, 10% O^+) was also tested, with 1000 uniformly spaced frequencies $0<\omega<2\omega_L$. In every case with $k^2>0$, the relation $(k^2)'>0$ was found to hold. Thus conditions (12) may be evaluated and used to limit the θ ranges of the integrals for diffusion coefficients.

V. DISCUSSION

As stated above, the resonance condition may be written in a variety of ways, and conditions analogous to Eq. (6) or Eq. (12) derived. Since all such methods only eliminate θ ranges that are known not to contain resonances, the computed diffusion coefficients should be unaffected, apart from considerations of efficiency and its practical converse, accuracy. However, variants of the method are not all equally effective.

Figure 6 illustrates conditions (6) and (12) for a 600 keV electron interacting of whistler waves with $\omega_{pe}^2/\Omega_e^2=0.3$. The plots are drawn for $\theta=30°$. In Figs. 6(a) and 6(b), the electron has $\alpha=25°$, the waves are taken to have $\omega_{LC}/\Omega_e=0.1$, $\omega_{UC}/\Omega_e=0.4$, and resonances with $n=1$ are considered. In Fig. 6(a), the minimum and maximum values of Ψ for these frequency cutoffs determine the shaded rectangle. Conditions (6), equivalent to V avoiding the rectangle, successfully identify the absence of the $n=1$ resonance for this θ. Figure 6(b) shows the same physical situation, but conditions (12) for $W(\omega)$ to avoid the rectangle determined by the minimum and maximum values of kc are not met, so the method fails to eliminate this nonresonant θ value. Figures 6(c) and 6(d) are similar, but with $\alpha=45°$, $\omega_{LC}/\Omega_e=0.05$, $\omega_{UC}/\Omega_e=0.2$, and

$n=-1$. Here, as shown in Fig. 6(c), the conditions in (6) are not met (the curve of V passes through the Ψ rectangle), so this θ value is unnecessarily kept, while Fig. 6(d) shows that conditions (12) are successful in identifying this θ as nonresonant (the curve of W avoids the kc rectangle).

The approach should be most effective when the resonance condition is written in a form $f(\omega,\theta)=g(\omega,\theta)$ with (say) f as weakly dependent on ω as possible, since when the curve of f is just a horizontal line, conditions relating the minimum and maximum values of f and g become exactly equivalent to the existence of resonances. [This is the case for $V(\omega)$ with $n=0$, which, for the whistler mode, often turns out to be particularly troublesome.]

Of course, it is also necessary to be able to locate the maximum and minimum of the two functions within ω_{LC} to ω_{UC}, with θ general, so that the conditions can be evaluated. So far this has been done for the resonance condition in the forms of Eqs. (5) and (11), where in each case both sides of the equation are either monotonic with respect to ω or else the product of two such factors (Ψ_1 and Ψ_2). Implementing both versions in a single computer code seems feasible and worthwhile, and probably also sufficient for any reasonable program of evaluating quasilinear diffusion coefficients.

Lyons[7] gave the general relation between pitch angle, energy, and cross diffusion coefficients: roughly, energy and cross diffusion become competitive with pitch angle diffusion when the resonant frequencies are not small compared to Ω_e. For whistler waves, the resonant frequency for a given particle tends to increase with decreasing ω_{pe}/Ω_e, even though this also decreases the maximum frequency at which whistlers can propagate.[3] Superluminous and Z-mode waves are compatible with ω as large as or larger than Ω_e, which again favors energy diffusion, even to the extent of exceeding pitch angle diffusion.[11] Decreasing ω_{pe}/Ω_e, especially below 1, also has the direct effect of enlarging the frequency range of propagation for the Z mode, and Summers *et al.*[10] found this parameter to be important for superluminous waves as well. The potential importance of these modes for pitch angle and energy diffusion of radiation belt electrons calls for more detailed evaluation of the diffusion rates, which awaits more comprehensive wave measurements.

ACKNOWLEDGMENT

This work was supported by the Space Vehicles Directorate of the Air Force Research Laboratory.

[1] J. M. Albert, J. Geophys. Res. **104**, 2429 (1999).
[2] J. M. Albert, J. Geophys. Res. **108**, 1249 (2003).
[3] J. M. Albert, J. Geophys. Res. **110**, A03218 (2005).
[4] R. B. Horne, R. M. Thorne, S. A. Glauert, J. M. Albert, N. P. Meredith, and R. R. Anderson, J. Geophys. Res. **110**, A03225 (2005).
[5] S. A. Glauert and R. B. Horne, J. Geophys. Res. **110**, A04206 (2005).
[6] N. P. Meredith, R. B. Horne, S. A. Glauert, R. M. Thorne, D. Summers, J. M. Albert, and R. R. Anderson, J. Geophys. Res. **111**, A05212 (2006).
[7] L. R. Lyons, J. Plasma Phys. **12**, 45 (1974).
[8] L. R. Lyons, J. Plasma Phys. **12**, 417 (1974).
[9] R. B. Horne and R. M. Thorne, Geophys. Res. Lett. **25**, 3011 (1998).
[10] D. Summers, R. M. Thorne, and F. Xiao, J. Geophys. Res. **106**, 10853 (2001).
[11] F. Xiao, H. He, Q. Zhou, H. Zheng, and S. Wang, J. Geophys. Res. **111**, A11201 (2006).
[12] D. Summers, J. Geophys. Res. **110**, A08213 (2005).
[13] Y. Y. Shprits, R. M. Thorne, R. B. Horne, and D. Summers, J. Geophys. Res. **111**, A10225 (2006).
[14] T. H. Stix, *Waves in Plasmas* (American Institute of Physics, New York, 1992).
[15] K. G. Budden, *The Propagation of Radio Waves* (Cambridge University Press, Cambridge, UK, 1985).
[16] J. M. Albert, Phys. Plasmas **11**, 4875 (2004).
[17] A. D. M. Walker, J. Plasma Phys. **18**, 339 (1977).
[18] A. D. M. Walker, *Plasma Waves in the Magnetosphere* (Springer-Verlag, Berlin, 1993).
[19] D. Summers, B. Ni, and N. P. Meredith, J. Geophys. Res. **112**, A04207 (2007).